Cancer Biomarkers 39 (2024) 231–243
DOI 10.3233/CBM-230175
IOS Press

KLF5 inhibits the migration and invasion in cervical cancer cell lines by regulating SNAI1

Xinjian Qu[a,b,*], Chang Xu[a,b], Wenbo Yang[c], Qianqian Li[c], Simei Tu[c] and Chenghai Gao[a,b,*]
[a]*Institute of Marine Drugs, Guangxi University of Chinese Medicine, Nanning, Guangxi, China*
[b]*Guangxi Key Laboratory of Marine Drugs, Guangxi University of Chinese Medicine, Nanning, Guangxi, China*
[c]*School of Life and Pharmaceutical Sciences, Dalian University of Technology, Dalian, Liaoning, China*

Received 19 May 2023
Accepted 21 November 2023

Abstract.
BACKGROUND: Epithelial-mesenchymal transition (EMT) is an important biological process by which malignant tumor cells to acquire migration and invasion abilities. This study explored the role of KLF5 in the EMT process of in cervical cancer cell lines.
OBJECTIVE: Krüpple-like factor 5 (KLF5) is a basic transcriptional factor that plays a key role in cell-cycle arrest and inhibition of apoptosis. However, the molecular mechanism by which KLF5 mediates the biological functions of cervical cancer cell lines has not been elucidated. Here, we focus on the potential function of ELF5 in regulating the EMT process in *in vitro* model of cervical cancer cell lines.
METHOD: Western-blot and real-time quantitative PCR were used to detect the expression of EMT-related genes in HeLa cells. MTT assays, cell scratch and Transwell assays were used to assess HeLa cells proliferation and invasion capability. Using the bioinformatics tool JASPAR, we identified a high-scoring KLF5-like binding sequence in the SNAI1 gene promoter. Luciferase reporter assays was used to detect transcriptional activity for different SNAI1 promoter truncates.
RESULT: After overexpressing the KLF5 gene in HeLa cells, KLF5 not only significantly inhibited the invasion and migration of HeLa cells, but also increased the expression of E-cadherin and decreased the expression of N-cadherin and MMP9. In addition, the mRNA expression of upstream regulators of E-cadherin, such as SNAI1, SLUG, ZEB1/2 and TWIST1 was also decreased. Furthermore, KLF5 inhibiting the expression of the SNAI1 gene via binding its promoter region, and the EMT of Hela cells was promoted after overexpression of the SNAI1 gene.
CONCLUSION: These results indicate that KLF5 can downregulate the EMT process of HeLa cells by decreasing the expression of the SNAI1 gene, thereby inhibiting the migration and invasion of HeLa cervical cancer cells.

Keywords: KLF5, EMT, SNAI1, cervical cancer cells

1. Introduction

Cervical cancer is one of the most common gynaecological malignancies, and its prevention has changed dramatically over the past decade [1]. With the development of vaccines and screening technologies, the incidence of cervical diseases has begun to decline in some countries [2]. However, extensive implementation has been restricted by economic factors and regional medical conditions [3]. The high incidence of carcinoma in situ is between 30 and 35 years old, and that of invasive cancer is between 45 and 55 years old, with a tendency of rejuvenation in recent years [4].

Histologic evaluation of cervical biopsy is the basis for the diagnosis of cervical cancer [5,6]. The two most common histopathologic types of cervical cancer include squamous cell carcinoma (up to 85% of cases) and adenocarcinoma (up to 25%), including adenosquamous carcinoma and other histopathologic

*Corresponding authors: Xinjian Qu and Chenghai Gao, Institute of Marine Drugs, Guangxi University of Chinese Medicine, Nanning, Guangxi 530200, China. E-mail: quxinjian@dlut.edu.cn and gaoch@gxtcmu.edu.cn.

types (6%) [7,8,9,10]. Cervical cancer stage is the most important prognostic factor, followed by nodal status, tumor volume, depth of cervical stromal infiltration, and lymphovascular interstitial infiltration [10]. Women with pelvic or paraaortic nodal involvement have a worse prognosis [11]. Therefore, effective therapies for this deadly disease are limited, as the molecular mechanisms underlying the progression of cervical cancer remain largely unknown. Several reports suggest that the aggressiveness of human cervical cancer is associated with a number of molecular abnormalities, including inactivation of various tumor suppressor genes and activation of various oncogenes [12,13,14]. Insufficient genetic and epigenetic data on the pathogenesis of cervical cancer and the lack of effective targets have hampered the development of novel targeted therapies [13, 14].

Cervical cancer metastasis involves a variety of signal transduction pathways and the epithelial-mesenchymal transformation (EMT) process [15,16, 17]. EMT refers to the morphological transformation of polarized epithelial cells into moving mesenchymal cells, which mainly manifests as reduced expression levels of the epithelial markers E-cadherin and keratin but increased expression level of mesenchymal-like markers such as vimentin, N-cadherin and matrix metalloproteinases (MMPs) along with enhanced migration ability [16,17,18]. EMT provides epithelial cells with different features associated with tumorigenesis because on EMT, cells become more motile and invasive, become more resistant to pro-apoptotic stimuli, reprogram their metabolism, and acquire characteristics of cancer stem cells [19]. Thus, EMT has attracted the attention of many cancer biologists and has been extensively studied in recent years. In addition, there are three main types of transcription factors: SNAI1, ZEB1/2 and bHLH (including TWIST1/2), which regulate the EMT process by affecting downstream gene expression levels [20,21,22]. SNAI1 is a zinc-finger transcription factor that can specifically recognize E-box elements on the E-cadherin promoter, thereby downregulating E-cadherin expression [20]. Moreover, it can downregulate cytokeratins, claudin, occludin, desmoplakin and plakophilin and upregulate N-cadherin, fibronectin, vitronectin, vimentin, MMPs, collagen, TWIST, ZEB1/2, etc. [23,24,25].

The Krüppel-like factor (KLF) family is a class of evolutionarily conserved transcription factors that is involved in multiple biological processes and diverse diseases, especially cancers [26]. The distinguishing feature of the KLF family is that the C-terminus of family members contains three conserved Cys2/His2 (C2H2) zinc-finger domains that bind to CACCC elements of DNA and GC-rich regions to activate or inhibit target gene transcription [27]. Krüppel-like factor 5 (KLF5), also known as BTEB2 or IKLF, is an important transcription factor that can regulate cell proliferation, differentiation, cell reprogramming, and autophagy [28, 29,30]. As a basic transcription factor, KLF5 regulates the expression of a wide range of downstream target genes, such as Nanog, STAT3 and COX2 [31,32,33]. For the past decade, KLF5 has been reported to participate in various biological functions, such as self-renewal of stem cells, proliferation, migration, and invasion [30,34]. Several outstanding articles have reported KLF5 plays vital roles in disease development, especially in cancers and cardiovascular diseases [29, 35]. However, the function of KLF5 in cervical cancer tumorigenesis has not been further studied. This study explores the role of KLF5 in the EMT process of cervical cancer cell lines and helps to support novel clues for future treatment in cervical cancer.

2. Materials and methods

2.1. Cell culture and reagents

Human cervical cancer HeLa cells, human cervical squamous cell carcinoma SiHa cells, C33A cells and COS-7 cells were obtained from the ATCC cell bank. The cells were cultured with Dulbecco's Modified Eagle's Medium (DMEM, Gibco, USA) containing 10% fetal bovine serum (FBS, Gibco, USA) and 1% penicillin-streptomycin (Thermo Scientific, USA) in an incubator at 37°C with humidified 5% CO_2.

2.2. Cell viability assays

MTT assays and colony formation assays were used to assess cellular viability. Twenty-four hours after transfection, cells were digested by trypsinization and then seeded in 96-well plates with 2×10^3 cells per well. In the MTT experiment, six groups were prepared, each with eight replicates. A group of cells was selected every 24 hours to detect cell viability by the MTT method. The absorbance of 450 nm wavelength was determined by a Microplate Reader (Bio Tek Instruments, Winooski, VT, USA). The MTT assay was performed following the manufacturer's protocol.

2.3. Cell migration and invasion assays

Cell migration and invasion assays were performed

Table 1
Sequence of primers used in this study

Gene		Sequence
KLF5	Forword	5'-ACAGTGCCTCAGTCGTAGACCAG-3'
KLF5	Reverse	5'-GCCAGTTCTCAGGTGAGTGATGTC-3'
SNAI1	Forword	5'-CCTCGCTGCCAATGCTCATCTG-3'
SNAI1	Reverse	5'-ACTGAAGTAGAGGAGAAGGACGAAGG-3'
SLUG	Forword	5'-CTGTGACAAGGAATATGTGAGC-3'
SLUG	Reverse	5'-CTAATGTGTCCTTGAAGCAACC-3'
ZEB1	Forword	5'-CAGGCAAAGTAAATATCCCTGC-3'
ZEB1	Reverse	5'-GGTAAAACTGGGGAGTTAGTCA-3'
ZEB2	Forword	5'-GAAGACAGAGAGTGGCATGTAT-3'
ZEB2	Reverse	5'-GTGTGTTCGTATTTATGTCGCA-3'
TWIST1	Forword	5'-GAAGACAGAGAGTGGCATGTAT-3'
TWIST1	Reverse	5'-GTGTGTTCGTATTTATGTCGCA-3'
E-cadherin	Forword	5' AGTCACTGACACCAACGATAAT-3'
E-cadherin	Reverse	5'-ATCGTTGTTCACTGGATTTGTG-3'
N-cadherin	Forword	5'-CGATAAGGATCAACCCCATACA-3'
N-cadherin	Reverse	5'-TTCAAAGTCGATTGGTTTGACC-3'
MMP9	Forword	5'-TCTGCCAGGACCGCTTCTACTG-3'
MMP9	Reverse	5'-GCAGGATGTCATAGGTCACGTAGC-3'
VIM	Forword	5'-ATGTCCACCAGGTCCGTGT-3'
VIM	Reverse	5'-TTCTTGAACTCGGTGTTGATGG-3'

as follows. After 24 hours of cell transfection, the cells were digested and suspended in serum-free medium. Suspended cells (1×10^5) were seeded in 24-well plates coated with Matrigel (BD Biosciences, CA) (invasion) or without Matrigel (migration) in the upper compartment with 8 μm pore polycarbonate membranes containing 100 μl FBS-free DMEM, and the lower compartment was supplemented medium with 20% FBS. After 24 h of incubation, non-migrated or non-invaded cells across the membranes were carefully removed with cotton swabs, while cells across the membrane were fixed with 4% paraformaldehyde and then stained by using the crystal violet dye. After that, cells were calculated under a microscope. The experiments to assess migrating and invading cells for each category of cells were repeated three times.

2.4. Wound-healing assays

Scratch wound-healing assays were performed as previously described [11]. In order to define migration ability of the human cervical cancer cells, cells were seeded onto 6-well plates and allowed to grow until to more than 90% confluence. The artificial gap was scratched by a 200 ml yellow pipette tip to create. The wound area was photographed by a phase-contrast microscope (Olympus CK30, Tokyo, Japan) at 0 h and 24 h after scratching, respectively. Then, the images were analyzed by ImageJ software 1.35 (NIH, Bethesda, MD, USA). The migratory rate was calculated by use of the following formula: (scratch width at 0 h-scratch width at 24 h)/scratch width at 0 h.

2.5. Reverse transcription and qPCR

Cells were washed twice with ice-cold PBS after 24 hours of transfection. Total RNA was extracted with TRIzol reagent (Invitrogen Thermo Fisher, USA), precipitated with isopropanol, and treated with DNase I (Ambion). cDNA synthesis was performed using the High-Capacity RNA-to-cDNA Kit (Takara, Dalian, China). qPCR analysis was performed using SYBR Green (Takara, Dalian, China) and the CFX96 Real-Time PCR detection system (Bio-Rad). PCR primer sequences are shown in Supplemental Table 1. GAPDH was used as an internal control, and three replicate wells were prepared for each sample. The expression (E) of each target mRNA relative to 18S rRNA was calculated based on the cycle threshold (Ct) as $E = 2^{-\Delta(\Delta Ct)}$, in which ΔCt = Ct (target) – Ct (18S), and $\Delta(\Delta Ct) = \Delta Ct$ (test sample) – ΔCt (control sample). For real time PCR, thermal cycling conditions were as follows: 95°C for 10 min, followed by 40 cycles of 95°C for 30 sec and 60°C for 1 min.

2.6. Plasmid and siKLF5 sequences

Complementary DNA encoding the full-length KLF5 gene was amplified by PCR and subcloned into pcDNA-3.1 plasmid containing Flag sequences. Similarly, full-length Snail complementary DNA was cloned into an N1 plasmid containing GFP sequences. The siKLF5#1 sequences were as follows: 5'-GCAGACUGCAGUGA AACAATT-3' (sense), 5'-UUGUUUCACUGCAGUCU

Table 2
Primer sequence for pGL3-SNAI1-Luc construction

Primer	Sequence
SNAI1-Luc-1K-Sense	5'-GGGTACCCGCAGTTGCCACTTCTT-3'
SNAI1-Luc-1K-Antisense	5'-CCAAGCTTGGGCTCGCTGTAGTTAGG-3'
SNAI1-Luc-500-Sense	5'-GGGTACCCCGGGGGCGGGCGTCGG-3'
SNAI1-Luc-500-Antisense	5'-CCAAGCTTGGGCTCGCTGTAGTTAGG-3'
SNAI1-Luc-300-Sense	5'-GGGTACCCGGACAGCCCCAGCACC-3'
SNAI1-Luc-300-Antisense	5'-CCAAGCTTGGGCTCGCTGTAGTTAGG-5'
SNAI1-Luc-200-Sense	5'-GGGTACCCGCGGAGGTGACAAAGG-3'
SNAI1-Luc-200-Antisense	5'-CCAAGCTTGGGCTCGCTGTAGTTAGG-3'
SNAI1-Luc-100-Sense	5'-CGGGGTACCCCGTAAGGGAGTTGGCGGC-3'
SNAI1-Luc-100-Antisense	5'-CCAAGCTTGGGCTCGCTGTAGTTAGG-3'

GCTT-3' (antisense); the siKLF5#2 sequences were as follows: 5'-GGCAAUUCACAAUCCAAAUTT-3' (sense), 5'-AUUUGGAUUGUGAA-UUGCCTT-3' (antisense); the siKLF5#3 sequences were as follows: 5'-GCAUCCACUA-CUGCGAUUATT-3' (sense), 5'-UAAUCGCAGUAGUGG-AUGCTT-3' (antisense); and the NC sequences were as follows: 5'-UUCUCCG AACGUGUCACGUTT-3' (sense), 5'-ACGUGACAC GUU-CGGAGAATT-3' (antisense).

2.7. Western blotting

The Western blot assay was conducted as follows. Briefly, 24 hours after transfection, the cells were washed twice with phosphate-buffered saline (PBS), supplemented with an appropriate amount of RIPA lysate, lysed at 4°C for 30 min, centrifuged at 12000 r/min for 10 min at 4°C, and the supernatant contained the total extracted protein. Electrophoresis was performed with a 10% concentration polyacrylamide gel (SDS-PAGE), and the proteins were transferred to PVDF membranes. The membranes were blocked in 5% milk and incubated with the primary antibodies at 4°C overnight. Primary antibodies contain: rabbit anti-KLF5 antibody and rabbit anti-SNAI1 antibody (Abcam, Cambridge, MA, USA); rabbit anti-Flag antibody (Sigma, MO, USA); mouse anti-E-cad, anti-N-cad and anti-GAPDH antibodies (Santa Cruz, CA, USA). Then, the membranes were washed with TBST, and were incubated with secondary antibodies at 37°C for one and a half hours. Finally, bands were visualized by using enzyme-linked chemiluminescence detection kit (ECL) assay and imaging by using the BioSpectrum Imaging System. GAPDH was used as a control, and the test was repeated at least three times.

2.8. Luciferase reporter assay

The JASPER database was used to predict the KLF5 binding site of the SNAI1 promoter region, and the pGL3 plasmid and SNAI1 promoter luciferase reporter gene plasmids of different lengths were constructed accordingly. The primer sequences used for SNAI1 luciferase reporter construction are listed in Table 2. Luciferase assays were performed on cell extracts according to the manufacturer's protocol. Briefly, COS-7 cells were transiently cotransfected with a KLF5 plasmid, and a human SNAI1 promoter reporter plasmid containing firefly luciferase that was expressed from CMV constitutive promoters. Twenty-four hours after transfection, cells were harvested, split equally among tubes, centrifuged, and resuspended to 3.4×10^5 cells/ml in media supplemented with 10% FBS, with the exception of passive lysis buffer, which was incubated with the cells for 15 min. Measures of 80 μL of cells were added to the wells of a 96-well plate, and 80 μL of ONE-GloTM EX reagent (Promega, Beijing, China) was added to each well. Next, 80 μL of NanoDLRTM Stop & Glo reagent (Promega, Beijing, China) was added to the wells containing NanoLuc luciferase. Luminescence was measured periodically over 3 hours. All experiments were repeated at least three times.

2.9. The SNAI1 gene expression, survival time and survival status of TCGA dataset

RNA-sequencing expression (level 3) profiles and corresponding clinical information for SNAI1 were downloaded from the TCGA dataset (https://portal.gdc.com). Log-rank test was used to compare differences in survival between these groups. The timeROC (v 0.4) analysis was used to compare the predictive accuracy of SNAI1 mRNA.

For Kaplan-Meier curves, p-values and hazard ratio (HR) with 95% confidence interval (CI) were generated by log-rank tests and univariate cox proportional hazards regression. All the analysis methods and R packages were implemented by R (foundation for statistical computing 2020) version 4.0.3. p value < 0.05 was considered statistically significant.

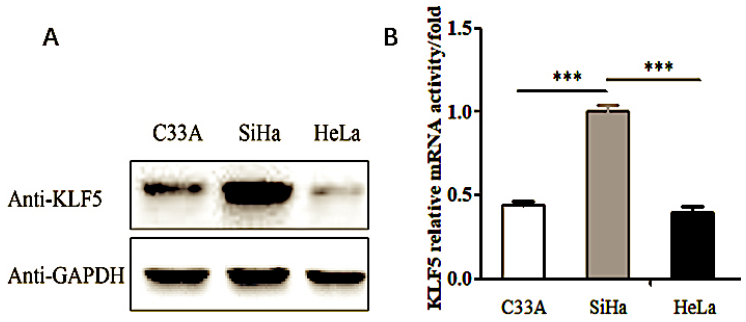

Fig. 1. The expression of KLF5 gene in the C33A, SiHa and HeLa cell lines. (A) Western blot analysis of the endogenous KLF5 protein expression level in the C33A, SiHa and HeLa cell lines. (B) Real-time PCR showing the KLF5 gene mRNA expression levels in the C33A, SiHa and HeLa cell lines.

2.10. Statistical analysis

The data are expressed as the means ± SDs from at least three independent experiments. The unpaired t-test method was used for comparisons between groups. Statistical analyses were carried out by one-way analysis of variance with Bonferroni's multiple-comparison correction for comparisons among three or more groups. The following labels were used: ns, not significant; *, $p < 0.05$; **, $p < 0.01$; and $^{***}p < 0.001$. GraphPad Prism 5.0 software was used for statistical analysis and graphing.

3. Results

3.1. Overexpression of KLF5 inhibited HeLa cell migration and invasion

To understand the function of KLF5 in the cervical cancer cell migration and invasion process, we searched the Human Protein Atlas database and found that KLF5 was expressed at low levels in HeLa cells and at high levels in SiHa cells. This conclusion has been verified at both the translational and transcriptional level. As shown in Fig. 1A and B, endogenous expression of the KLF5 gene was detected in three cell lines, HeLa, SiHa and C33A, using Western blot and real-time PCR methods. The expression of KLF5 identified in SiHa cells was relatively higher than that in HeLa cells and C33A cells ($p < 0.001$). Therefore, HeLa cells and SiHa cells were selected in subsequent experiments.

KLF5 was overexpressed in HeLa cells, and the effect on cell viability, cell migration and invasion were observed. In the MTT assay, when the KLF5 gene was overexpressed, the viability of HeLa cells was not obviously affected ($p > 0.05$) (Fig. 2A). However, in scratch wound-healing and Transwell assays, the overexpression of the KLF5 gene significantly inhibited HeLa cell migration and invasion ($p < 0.001$), respectively (Fig. 2B and C).

3.2. Overexpression of the KLF5 gene inhibits the EMT process in HeLa cells

Cell invasion and migration are a series of dynamic processes, which are often associated with EMT during cancer progression. The phenotypic characteristics in EMT include a loss of cell adhesion, acquisition of motility, and expression of EMT relative genes. To explore the molecular mechanism by which the transcription factor KLF5 regulates the EMT process in cervical cancer cells, EMT-related gene expression was detected by quantitative real-time PCR and Western blot experiments.

After the Flag-KLF5 plasmid was transfected into HeLa cells, the expression of E-cadherin, an epithelial-like cell marker, was increased ($p < 0.001$), while the expression of N-cadherin, a mesenchymal cell marker, and MMP9, a cell migration marker, was decreased ($p < 0.001$).

SNAI1, ZEB1/2 and TWIST are upstream regulatory factors of the E-cadherin protein (Fig. 3A). The transcription factor SNAI1 is an important participant in the EMT process and can bind to E-box elements in the E-cadherin promoter to inhibit its transcription. In addition, SNAI1 can also regulate SLUG, ZEB1, ZEB2, TWIST1, N-cadherin and MMP9 expression. After overexpressing KLF5 in HeLa cells, the expression levels of SNAI1, SLUG, ZEB1 and ZEB2 factors was significantly decreased ($p < 0.001$), and the TWIST1 transcription factors was also decreased ($p < 0.05$) (Fig. 3B and C).

Next, we explored whether the KLF5 gene regulates the expression of EMT-related molecules in cervical

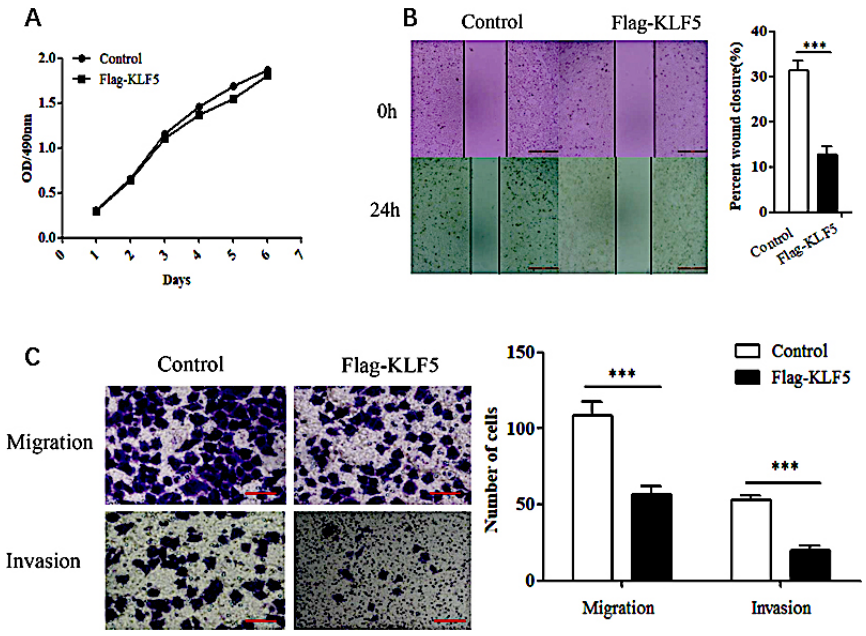

Fig. 2. The effects of KLF5 on the proliferation and motility of HeLa cells. (A) MTT assays assessing the effect of KLF5 overexpression on the proliferation of HeLa cells. (B) Scratch wound-healing assays evaluating the effect of KLF5 overexpression on the motility of HeLa cells. (C) Transwell assay evaluating the effect of KLF5 overexpression on the migration and invasion abilities of HeLa cells. The bar graphs show the numbers of migrating and invading cells from triplicate experiments (right).

cancer cells through the SNAI1 gene. Western blot experiments showed that after overexpression of the KLF5 gene in HeLa cells, E-cadherin expression was upregulated, while N-cadherin and SNAI1 expression was downregulated ($p < 0.01$) (Fig. 3D).

3.3. Silencing the KLF5 gene promotes EMT in SiHa cells

After silencing the KLF5 gene in SiHa cells with siRNA (Fig. 4A), the mRNA expression of EMT-related genes was assessed; the experiments revealed that the expression of the E-cadherin gene was reduced, and the expression of N-cadherin and MMP9 genes was increased (Fig. 4B). The upstream genes SNAI1, SNAI2, ZEB1, ZEB2, and TWIST1, which regulate the expression of E-cadherin, were increased. In particular, the expression of SNAI1 significant increased ($p < 0.01$) (Fig. 4C). Western blot experiments showed that the expression of E-cadherin was downregulated, and the expression of N-cadherin and SNAI1 was upregulated ($p < 0.01$) (Fig. 4D).

The above results indicate that the KLF5 gene can regulate the EMT process of cervical cancer cells and the expression levels of related genes, and may indirectly promote the EMT process by regulating the expression of SNAI1.

3.4. The KLF5 inhibits the SNAI1 expression

A characteristic feature of KLF5 is that its C-terminus contains three conserved C2H2 zinc-finger domains, which can recognize and bind to the 5'-CACCC-3' sequence and GC-rich regions in the promoters of target genes.

To further verify whether KLF5 regulates the EMT process of cervical cancer cells by inhibiting the expression of the SNAI1 gene, the bioinformatics database JASPER was used to predict KLF5 binding sites in the SNAI1 gene promoter region. The analysis of the simulation results revealed that the SNAI1 promoter contained multiple predicted KLF5 binding sites in the $-1000\sim+100$ sequence region (Fig. 5A). Based on these sites, truncated plasmids with different lengths of the SNAI1 promoter were constructed, which were denoted as SNAI1-Luc-1K, SNAI1-Luc-500, SNAI1-Luc-300, SNAI1-Luc-200 and SNAI1-Luc-100 (Fig. 5B).

A luciferase reporter gene was used to detect the effect of the KLF5 on the SNAI1 promoter region. The KLF5 had a significant inhibitory effect on SNAI1-Luc-1K, SNAI1-Luc-500, SNAI1-Luc-300, and SNAI1-Luc-200, with the highest inhibitory effect reaching 80% ($p < 0.001$). However, the inhibitory effect of KLF5 on SNAI1-Luc-100 was lower than the effect in the other constructs, and there was no significant dif-

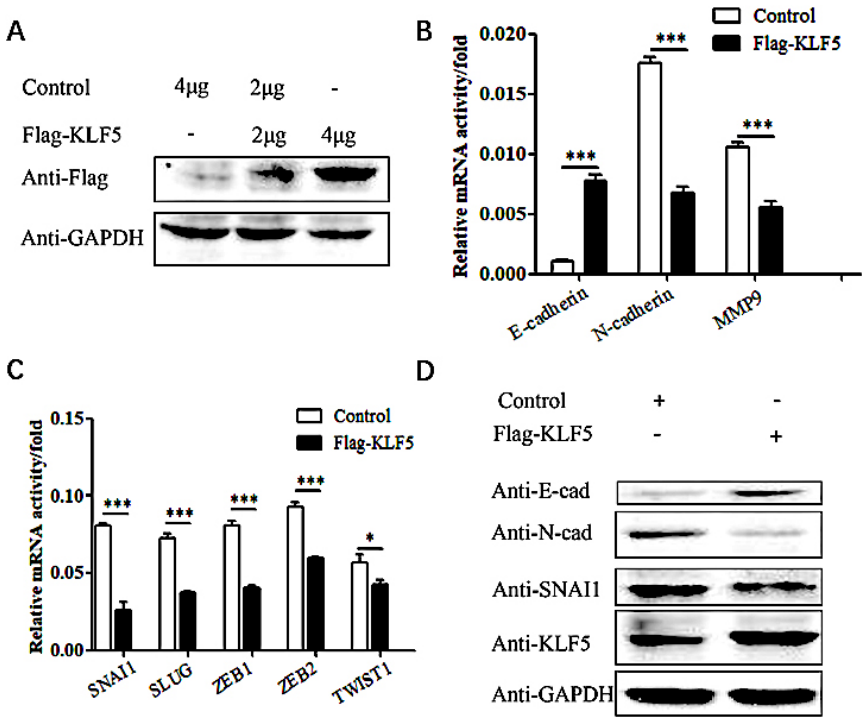

Fig. 3. The effect of KLF5 overexpression on the EMT phenotype in HeLa cells. (A) Western blot analysis of the exogenous KLF5 protein expression level in HeLa cells. (B) Real-time PCR showing the effect of KLF5 overexpression on the mRNA level of E-cadherin, N-cadherin and MMP9 in HeLa cells. The bar graphs show the fold changes in relative mRNA levels normalized against GAPDH. (C) Real-time PCR showing the effect of KLF5 overexpression on the mRNA level of SNAI1, SLUG, ZEB1, ZEB2 and TWIST1 in HeLa cells. The bar graphs show the fold changes in relative mRNA levels normalized against GAPDH. (D) Western blot analysis of the effect of KLF5 overexpression on the protein expression levels of E-cadherin, N-cadherin and SNAI1 in HeLa cells.

ference ($p > 0.05$) (Fig. 5C). This indicates that the -200 to -100 region of the SNAI1 promoter contains the binding site for KLF5, and the KLF5 can bind to the SNAI1 promoter region (-200 to -100) to inhibit the expression of the SNAI1 gene. To determine the inhibitory effect of the KLF5 on SNAI1-Luc-200, different concentration of the KLF5 gene were transfected into cells in a 24-well plate. As shown in Fig. 5D, the KLF5 inhibited the expression of SNAI1-Luc-200 in a dose-dependent manner ($p < 0.001$). The above results indicate that the KLF5 can bind to the -200 to -100 region upstream of the promoter of the SNAI1 gene to inhibit the expression of the SNAI1 gene.

3.5. *Overexpression of the SNAI1 gene inhibits the EMT process in HeLa cells*

To further verify that KLF5 regulates the migration and invasion abilities of cervical cancer cells through a SNAI1-mediated EMT process, the SNAI1 gene was overexpressed in HeLa cells, and the mRNA level of EMT-related genes was detected using real-time PCR technology. Overexpression of the SNAI1 gene inhibited the expression of the epithelial marker E-cadherin and promoted the expression of the mesenchymal markers N-cadherin and MMP9 ($p < 0.001$) (Fig. 6A). Overexpression of the SNAI1 gene also promoted the expression of its downstream transcription factors SLUG, ZEB1, ZEB2 and TWIST1 ($p < 0.001$) (Fig. 6B). Western blot experiments confirmed that overexpression of SNAI1 inhibited the expression of E-cadherin while promoting the expression of N-cadherin in HeLa cells ($p < 0.01$) (Fig. 6C). Therefore, the SNAI1 gene is a key transcription factor in the EMT process, and KLF5 regulation of SNAI1 affects the EMT process of cervical cancer cells.

3.6. *Prognostic value of the SNAI1 gene in cervical cancer*

Because SNAI1 gene often promotes a more aggressive tumor phenotype, we further investigated the prognostic value of the SNAI1 gene. As shown in the heatmap (Fig. 7A), the expressions of the SNAI1 genes

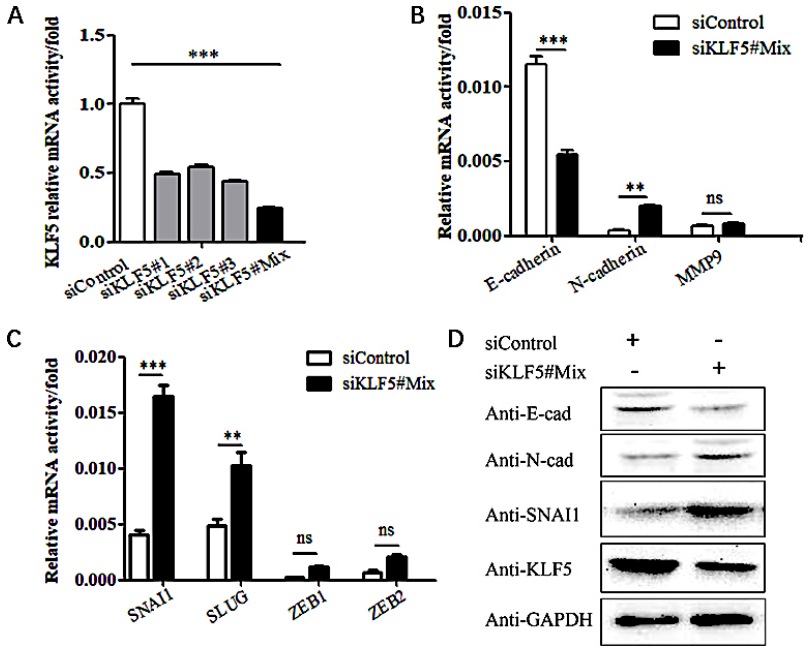

Fig. 4. The effect of silencing the KLF5 gene on the EMT phenotype in SiHa cells. (A) The efficacy of KLF5 silencing as validated by real-time PCR. (B) Real-time PCR showing the effect of KLF5 knockdown on the mRNA levels of E-cadherin, N-cadherin and MMP9 in SiHa cells. (C) Real-time PCR showing the effect of KLF5 knockdown on the mRNA levels of SNAI1, SLUG, ZEB1 and ZEB2 in SiHa cells. (D) Western blot analysis of the effect of silencing KLF5 on the protein expression levels of E-cadherin, N-cadherin and SNAI1 in SiHa cells.

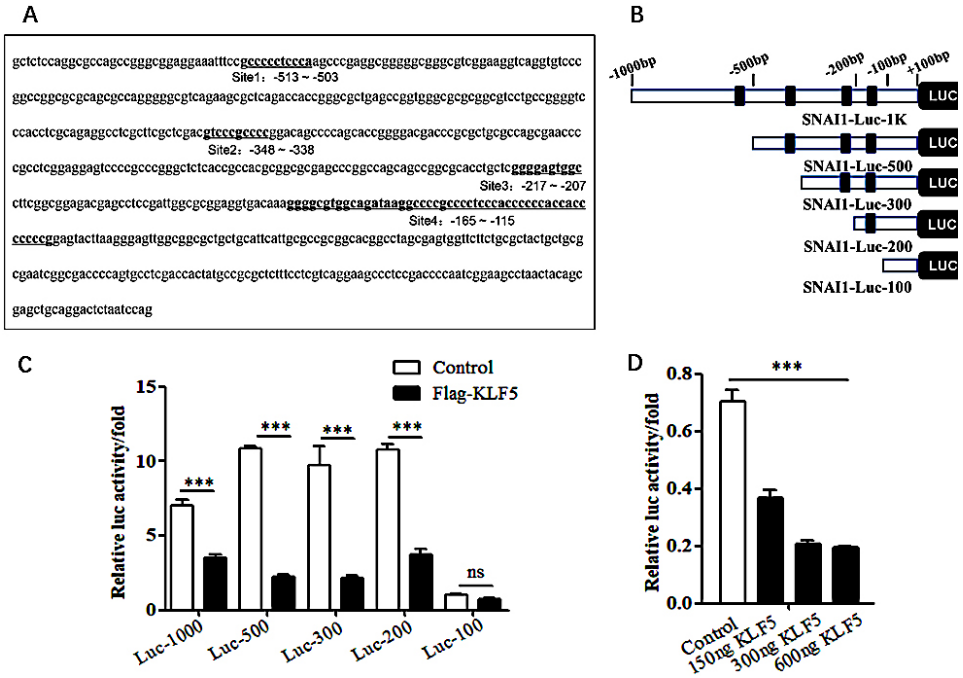

Fig. 5. Assessment of the effects of KLF5 on the activity of SNAI1 promoter. (A) JASPER database analysis of potential KLF5 binding sites in the SNAI1 promoter region. (B) Schematic illustrating the construction of a series of human SNAI1 promoter reporter plasmids. (C) Luciferase reporter gene experiment assessing the effect of the KLF5 on the activities of the SNAI1 constructs with different promoter truncations. (D) Luciferase reporter gene experiment assessing the effect of the KLF5 on the activity of the SNAI1-Luc-200 promoter at different concentrations.

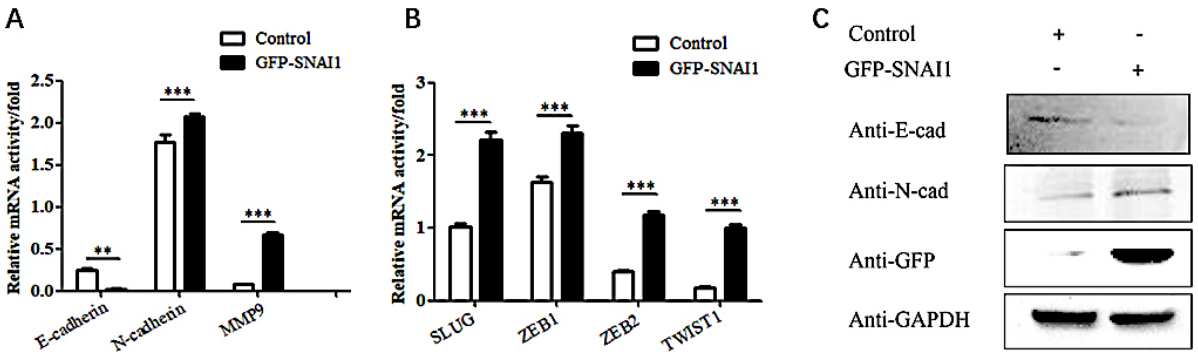

Fig. 6. The effects of overexpressing the SNAI1 gene on EMT phenotypes in HeLa cells. (A) Real-time PCR showing the effect of SNAI1 overexpression on the mRNA levels of E-cadherin, N-cadherin and MMP9 in HeLa cells. The bar graphs show the fold changes in relative mRNA levels normalized against GAPDH. (B) Real-time PCR showing the effect of SNAI1 overexpression on the mRNA levels of SNAI1, SLUG, ZEB1, ZEB2 and TWIST1 in HeLa cells. The bar graphs show the fold changes in relative mRNA levels normalized against GAPDH. (C) Western blot showing the effect of SNAI1 overexpression on the expression levels of E-cadherin, N-cadherin and GFP-SNAI1 in HeLa cells.

were increased accompanying higher risk scores in both the TCGA databases, implying that patients with high risk tend to survival status. Our data also showed that the mortality rate in the high-risk group was significantly higher than in the low-risk group (Fig. 7B).

To evaluate the predictive efficiency of the SNAI1 gene in the 1-, 3-, and 5-years survival rate, we performed a the received operating characteristic (ROC) curve utilizing the data from the TCGA datasets. The area under the ROC curve (AUC) was 0.569 at 1-year, 0.589 at 3-years, and 0.567 at 5-years, respectively, indicating a high predictive value (Fig. 7C).

4. Discussion

Cervical cancer is the third leading cause of cancer-related death in females after breast and colorectal cancers worldwide. Over 111,820 new cases and 13,740 cervical cancer deaths are estimated to occur in 2022 [36]. However, effective therapies for this deadly disease are limited because the elaborate molecular mechanism underlying cervical cancer progression remains unknown [3].

KLF5 has been reported to interact with multiple transcription factors in a variety of tumors by immunoprecipitation and mass spectrometry [34]. KLF5 can form transcriptional complexes with transcription-associated factors to regulate the transcription of target genes [30,32]. In estrogen receptor α (ERα) positive breast cancer cells, estrogen is an important cancer-promoting factor. KLF5 binds to ERα in breast cancer and inhibits the transcriptional activity of ERα [37]. In prostate cancer, KLF5 cooperates with estrogen receptor β (ERβ) to promote forkhead box O1 (FOXO1) transcription and suppress tumor growth [38]. In response to transforming growth factor-β (TGF-β), KLF5 forms a transcription complex with SMAD family member 2/3/4 (SMAD2/3/4) to activate the transcription of p15 and inhibit the transcription of c-Myc [39].

KLF5 regulates not only protein-coding genes but also the transcription of several miRNAs and long non-coding RNAs (lncRNAs) [40]. KLF5 could activates tumor necrosis factor receptor superfamily member 11a (TNFRSF11a) gene transcription by binding to the TNFRSF11a gene promoter in cervical cancer [41]. KLF5 increases oxidative stress by decreasing glutathione biosynthesis in B-cell lymphoid progenitor leukemogenesis [42]. In the context of p53 loss, KLF5 promotes miR-192 transcription, which inhibits the expression of zinc finger E-Box binding homeobox 2 (ZEB2) and EMT in liver cancer cells [43]. Additionally, KLF5 induces the transcription of miR-200 and inhibits the EMT process of epithelial cells [44]. This study took cervical cancer cells as the research target and found that the overexpression of KLF5 inhibited the migration and invasion of HeLa cells. A comparative study found that after silencing the KLF5 gene in SiHa cells, the expression of SNAI1, SLUG, ZEB1, ZEB2, and TWIST1 was upregulated, speculating that KLF5 can regulate the EMT process of cervical cancer cells through the TGF-β signaling pathway.

During the EMT process, the expression of various transcription factors changes. SNAI1/2 are zinc finger transcription factors that can specifically recognize the three CAGGTG or CACCTG E-box elements in the E-cadherin promoter, thereby downregulating E-cadherin expression [20]. Meanwhile, they can downregulate cytokeratins, claudin, occludin, desmoplakin and plakophilin, and upregulate N-cadherin, fibronectin,

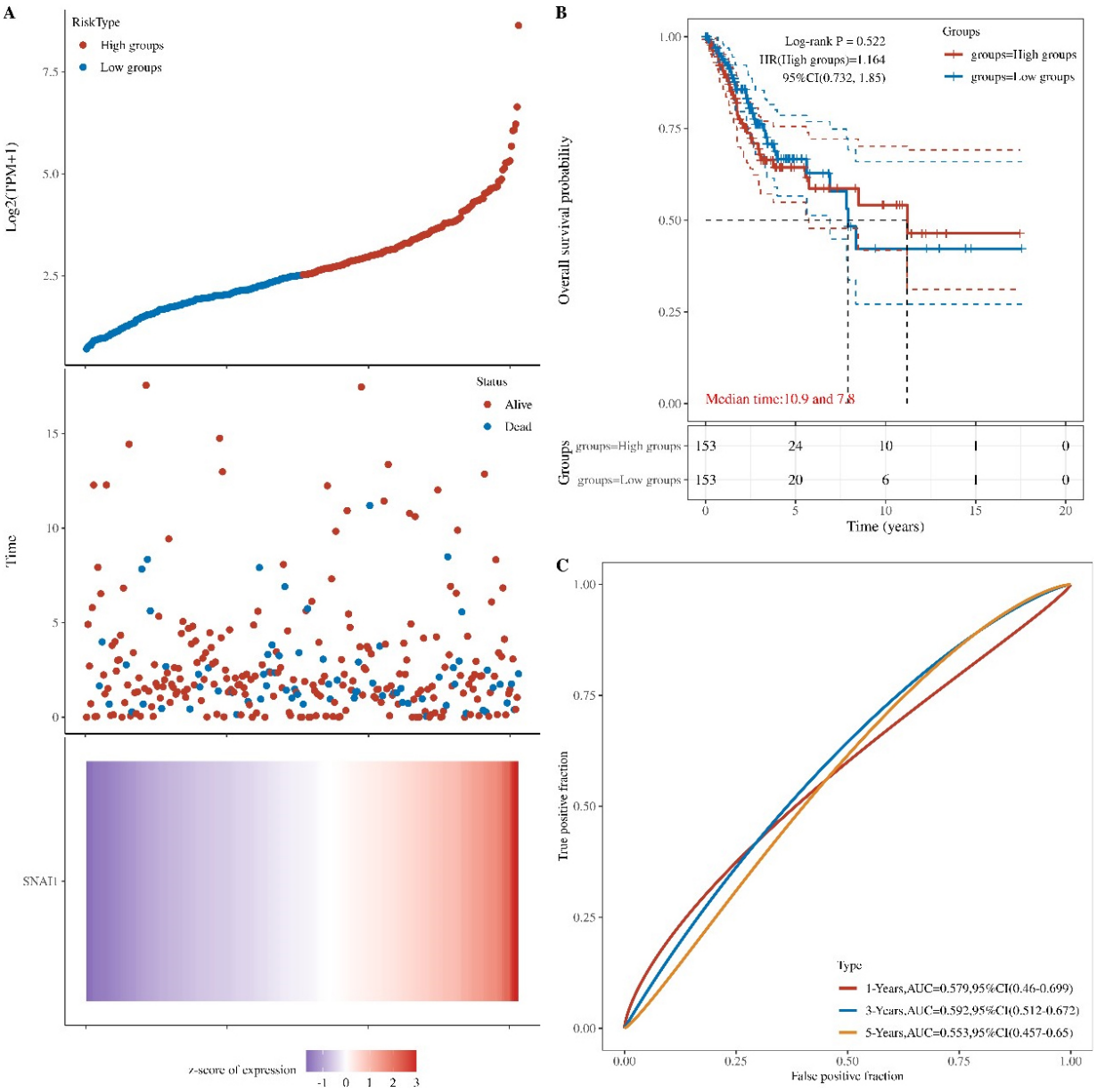

Fig. 7. Prognostic value of the SNAI1 gene in cervical cancer. (A) A heatmap showing SNAI1 gene expression profiles in cervical cancer from the TCGA databases. (B) The prognosis values of SNAI1 gene in TCGA data. (C) The prognosis values of SNAI1 gene in GBM in the TCGA data.

vitronectin, vimentin, MMPs, collagen, TWIST, and ZEB1/2 [20,21,22,23,24,25,45,46]. Studies have found that epidermal growth factor receptor (EGFR) is highly expressed in cervical cancer, and this overexpression causes the accumulation of SNAI1 in the cell nucleus by inhibiting glycogen synthase kinase-3β. In addition, high expression of TWIST can also activate the Akt signaling pathway, affecting glycogen synthase kinase-3β, thereby regulating the expression of SNAI1 and inhibiting the expression of E-cadherin [21]. High expression of ZEB1, MMP7 and MMP9 can promote the EMT process of serous ovarian tumors, thereby enhancing tumor invasion and metastasis [21,47,48].

In our study, silencing KLF5 with siRNA inhibited the expression of E-cadherin, promoted the expression of N-cadherin and MMP9, and upregulated the expression of the upstream transcription factor SNAI1 in SiHa cells. We investigated the role of KLF5 in regulating SNAI1 expression and found that the KLF5 could bind multiple sites of the SNAI1 promoter region

via the JASPER database analyses. KLF5 may bind to the $-200\sim-100$ region of the SNAI1 promoter region to inhibit SNAI1 expression. The results showed that KLF5 inhibited the expression of the SNAI1 by binding the SNAI1 promoter region, and the EMT process of Hela cells was promoted after overexpression of the SNAI1 gene.

5. Conclusion

Accumulating evidence from our laboratory has suggested an inhibitory effect of KLF5 on SNAI1 transcription in Hela cells. In addition, KLF5 upregulated E-cadherin expression and downregulated N-cadherin and MMP9. KLF5 also downregulated the expression EMT relative genes, such as SNAI1, ZEB1, ZEB2, and TWIST1, which is novel evidence underlying migration and invasion in a cell line of cervical carcinoma, Hela cells.

Acknowledgments

This work was supported by grants from Guangxi University of Chinese Medicine "GuiPai Traditional Chinese Medicine inheritance and innovation team" Project (2022A007), the Research Launching Fund Project from Guangxi University of Chinese Medicine Introduced the Doctoral (2022BS021) and the Fundamental Research Funds for the Central of China (DUT20JC25).

Author contributions

For every author, his or her contribution to the manuscript needs to be provided using the following categories:
Conception: Chang Xu, Wenbo Yang.
Interpretation or analysis of data: Chang Xu, Wenbo Yang, Qianqian Li, Simei Tu.
Preparation of the manuscript: Xinjian Qu, Chenghai Gao.
Revision for important intellectual content: Chang Xu, Wenbo Yang, Xinjian Qu.
Supervision: Xinjian Qu, Chenghai Gao.

Conflict of interest

The authors declare that they have no conflict of interest.

References

[1] A. Gupta, A. Parveen, A. Kumar and P. Yadav, Advancement in deep learning methods for diagnosis and prognosis of cervical cancer, *Curr Genomics* **23** (2022), 234–245. doi: 10.2174/1389202923666220511155939.

[2] D. Miller, C.P. Morris, Z. Maleki, M. White and E.F. Rodriguez, Health disparities in cervical cancer: Prevalence of high-risk HPV and cytologic diagnoses according to race, *Cancer Cytopathol* **128** (2020), 860–869. doi: 10.1002/cncy.22316.

[3] M. Schubert, D.O. Bauerschlag, M.Z. Muallem, N. Maass and I. Alkatout, Challenges in the diagnosis and individualized treatment of cervical cancer, *Medicina (Kaunas)* **59** (2023), 925. doi: 10.3390/medicina59050925.

[4] R.L. Siegel, K.D. Miller, H.E. Fuchs and A. Jemal, Cancer statistics, 2022, *CA Cancer J Clin* **72** (2022), 7–33. doi: 10.3322/caac.21708.

[5] C. Gnade, E.K. Hill, H. Botkin, A. Hefel, H. Hansen, S.L. Mott, A. Hardy-Fairbanks and C. Stockdale, Is the age of cervical cancer diagnosis changing over time? *J Gynecol Obstet Hum Reprod* **50** (2021), 102040. doi: 10.1016/j.jogoh.2020.102040.

[6] H.E.G. Ghaleh, A. Shahriary, M. Izadi and M. Farzanehpour, Advances in early diagnosis of cervical cancer based on biosensors, *Biotechnol Bioeng* **119** (2022), 2305–2312. doi: 10.1002/bit.28149.

[7] A.J.B. Smith, A.L. Beavis, A.F. Rositch and K. Levinson, Disparities in diagnosis and treatment of cervical adenocarcinoma compared with squamous cell carcinoma: An analysis of the national cancer database, 2004–2017, *J Low Genit Tract Dis* **27** (2023), 29–34. doi: 10.1097/LGT.0000000000000702.

[8] A. Macios, K. Komerska and A. Nowakowski, Reasons for truly negative cytology reports preceding the diagnoses of invasive cervical cancer-results of a false-negative cytology audit in polish cervical cancer screening programme, *Cancer Med* **12** (2023), 13800–13810. doi: 10.1002/cam4.6024.

[9] A.J.B. Smith, A.L. Beavis, A.F. Rositch and K. Levinson, Disparities in diagnosis and treatment of cervical adenocarcinoma compared with squamous cell carcinoma: An analysis of the national cancer database, 2004–2017, *Journal of Lower Genital Tract Disease* **27** (2023), 29–34. doi: 10.1097/Lgt.0000000000000702.

[10] D.B. Vale, C. Sauvaget, R. Muwonge, L.C.S. Thuler, P. Basu, L.C. Zeferino and R. Sankaranarayanan, Level of human development is associated with cervical cancer stage at diagnosis, *J Obstet Gynaecol* **39** (2019), 86–90. doi: 10.1080/01443615.2018.1463976.

[11] S. Padavu, P. Aichpure, B.K. Kumar, A. Kumar, R. Ratho, S. Sonkusare, I. Karunasagar, I. Karunasagar and P. Rai, An insight into clinical and laboratory detections for screening and diagnosis of cervical cancer, *Expert Rev Mol Diagn* **23** (2023), 29–40. doi: 10.1080/14737159.2023.2173580.

[12] L.B. Bateman, S. Blakemore, A. Koneru, T. Mtesigwa, R. McCree, N.F. Lisovicz, E.A. Aris, S. Yuma, J.D. Mwaiseiage and P.E. Jolly, Barriers and facilitators to cervical cancer screening, diagnosis, follow-up care and treatment: Perspectives of human immunodeficiency virus-positive women and health care practitioners in tanzania, *Oncologist* **24** (2019), 69–75. doi: 10.1634/theoncologist.2017-0444.

[13] S.Z. Wang, B. Ding, S.Y. Wang, W.J. Yan, Q.Q. Xia, D. Meng, S.Q. Xie, S.Y. Shen, B.J. Yu, H.H. Liu, J. Hu and X. Zhang, Gene signature of m⁶A RNA regulators in diagnosis, prognosis, treatment, and immune microenvironment for cervical cancer, *Sci Rep* **12** (2022), 17667. doi: 10.1038/s41598-022-22211-2.

[14] S. Shen, S. Zhang, P. Liu, J. Wang and H. Du, Potential role of microRNAs in the treatment and diagnosis of cervical cancer, *CancernGenet* **248-249** (2020), 25–30. doi: 10.1016/j.cancergen.2020.09.003.

[15] R. Qureshi, H. Arora and M.A. Rizvi, EMT in cervical cancer: Its role in tumour progressio and response to therapy, *Cancer Lett* **356** (2015), 321–331. doi: 10.1016/j.canlet.2014.09.021.

[16] L. Wu, L. Han, C. Zhou, W. Wei, X. Chen, H. Yi, 2015, X. Wu, X. Bai, S. Guo, Y. Yu, L. Liang and W. Wang, TGF-beta1-induced CK17 enhances cancer stem cell-like properties rather than EMT in promoting cervical cancer metastasis via the ERK1/2-MZF1 signaling pathway, *FEBS J* **284** (2017), 3000–3017. doi: 10.1111/febs.14162.

[17] X.H. Wang, X. He, H.Y. Jin, J.X. Liang and N. Li, Effect of hypoxia on the Twist1 in EMT of cervical cancer cells, *Eur Rev Med Pharmacol Sci* **22** (2018), 6633–6639. doi: 10.26355/eurrev_201810_16138.

[18] H.Y. Liu, Z.Y. Zhu, X.M. Chen, J.Q. Lu, Y. Song and W. Xia, A review of the effects of estrogen and epithelial-mesenchymal transformation on intrauterine adhesion and endometriosis, *Transpl Immunol* **79** (2023), 101679. doi: 10.1016/j.trim.2022.101679.

[19] I. Nagle, A. Richert, M. Quinteros, S. Janel, E. Buysschaert, N. Luciani, H. Debost, V. Thevenet, C. Wilhelm, C. Prunier, F. Lafont, T. Padilla-Benavides, M. Boissan and M. Reffay, Surface tension of model tissues during malignant transformation and epithelial-mesenchymal transition, *Front Cell Dev Biol* **10** (2022), 926322. doi: 10.3389/fcell.2022.926322.

[20] D. Singh, R.K. Deshmukh and A. Das, SNAI1-mediated transcriptional regulation of epithelial-to-mesenchymal transition genes in breast cancer stem cells, *Cell Signal* **87** (2021), 110151. doi: 10.1016/j.cellsig.2021.110151.

[21] Z.L. Chen, S. Li, K.C. Huang, Q.H. Zhang, J. Wang, X. Li, T. Hu, S.S. Wang, R. Yang, Y. Jia, H.Y. Sun, F.X. Tang, H. Zhou, J. Shen, D. Ma and S.X. Wang, The nuclear protein expression levels of SNAI1 and ZEB1 are involved in the progression and lymph node metastasis of cervical cancer via the epithelial-mesenchymal transition pathway, *Hum Pathol* **44** (2013), 2097–2105. doi: 10.1016/j.humpath.2013.04.001.

[22] M. Han and W.P. Xu, EMP3 is induced by TWIST1/2 and regulates epithelial-to-mesenchymal transition of gastric cancer cells, *Tumour Biol* **39** (2017), 1010428317718404. doi: 10.1177/1010428317718404.

[23] G. Tao, L.J. Miller and J. Lincoln, Snai1 is important for avian epicardial cell transformation and motility, *Dev Dyn* **242** (2013), 699–708. doi: 10.1002/dvdy.23967.

[24] D.S. Al-Hattab, H.A. Safi, R.S. Nagalingam, R.A. Bagchi, M.T. Stecy and M.P. Czubryt, Scleraxis regulates Twist1 and Snai1 expression in the epithelial-to-mesenchymal transition, *Am J Physiol Heart Circ Physiol* **315** (2018), H658–H668. doi: 10.1152/ajpheart.00092.2018.

[25] A. Jouppila-Matto, M. Närkiö-Mäkelä, Y. Soini, M. Pukkila, R. Sironen, H. Tuhkanen, A. Mannermaa and V.M. Kosma, Twist and snai1 expression in pharyngeal squamous cell carcinoma stroma is related to cancer progression, *Bmc Cancer* **11** (2011), 350. doi: 10.1186/1471-2407-11-350.

[26] B.B. McConnell and V.W. Yang, Mammalian Kruppel-like factors in health and diseases, *Physiol Rev* **90** (2010), 1337–1381. doi: 10.1152/physrev.00058.2009.

[27] Y. Zhang, C. Yao, Z. Ju, D. Jiao, D. Hu, L. Qi, S. Liu, X. Wu and C. Zhao, Kruppel-like factors in tumors: Key regulators and therapeutic avenues, *Front Oncol* **13** (2023), 1080720. doi: 10.3389/fonc.2023.1080720.

[28] H. Cao, G. Pan, S. Tang, N. Zhong, H. Liu, H. Zhou, Q. Peng and Y. Zou, miR-145-5p regulates the proliferation, migration and invasion in cervical carcinoma by targeting KLF5, *Onco Targets Ther* **13** (2020), 2369–2376. doi: 10.2147/OTT.S241366.

[29] E. Lee, J. Cheung and A.B. Bialkowska, Kruppel-like Factors 4 and 5 in Colorectal Tumorigenesis, *Cancers (Basel)* **15** (2023), 2430. doi: 10.3390/cancers15092430.

[30] M.O. Nandan, A.M. Ghaleb, A.B. Bialkowska and V.W. Yang, Kruppel-like factor 5 is essential for proliferation and survival of mouse intestinal epithelial stem cells, *Stem Cell Research* **14** (2015), 10–19. doi: 10.1016/j.scr.2014.10.008.

[31] S. Parisi and T. Russo, Regulatory role of Klf5 in early mouse development and in embryonic stem cells, *Vitam Horm* **87** (2011), 381–397. doi: 10.1016/B978-0-12-386015-6.00037-8.

[32] J.B. Ma, J.Y. Bai, H.B. Zhang, J. Jia, Q. Shi, C. Yang, X. Wang, D. He and P. Guo, KLF5 inhibits STAT3 activity and tumor metastasis in prostate cancer by suppressing IGF1 transcription cooperatively with HDAC1, *Cell Death Dis* **11** (2020), 466. doi: 10.1038/s41419-020-2671-1.

[33] L. Zhang, Y. Wu, J. Wu, M. Zhou, D. Li, X. Wan, F. Jin, Y. Wang, W. Lin, X. Zha and Y. Liu, KLF5-mediated COX2 up-regulation contributes to tumorigenesis driven by PTEN deficiency, *Cell Signal* **75** (2020), 109767. doi: 10.1016/j.cellsig.2020.109767.

[34] Y. Luo and C. Chen, The roles and regulation of the KLF5 transcription factor in cancers, *Cancer Sci* **112** (2021), 2097–2117. doi: 10.1111/cas.14910.

[35] R.M. Di, C.X. Yang, C.M. Zhao, F. Yuan, Q. Qiao, J.N. Gu, X.M. Li, Y.J. Xu and Y.Q. Yang, Identification and functional characterization of KLF5 as a novel disease gene responsible for familial dilated cardiomyopathy, *Eur J Med Genet* **63** (2020), 103827. doi: 10.1016/j.ejmg.2019.103827.

[36] C.F. Xia, X.S. Dong, H. Li, M.M. Cao, D.A.Q. Sun, S.Y. He, F. Yang, X.X. Yan, S.L. Zhang, N. Li and W.Q. Chen, Cancer statistics in China and United States, 2022: Profiles, trends, and determinants, *Chin Med J (Engl)* **135** (2022), 584–590. doi: 10.1097/CM9.0000000000002108.

[37] P. Guo, X.Y. Dong, K.W. Zhao, X.D. Sun, Q.N. Li and J.T. Dong, Estrogen-induced interaction between KLF5 and estrogen receptor (ER) suppresses the function of ER in ER-positive breast cancer cells, *Int J Cancer* **126** (2010), 81–89. doi: 10.1002/ijc.24696.

[38] Y. Nakajima, A. Osakabe, T. Waku, T. Suzuki, K. Akaogi, T. Fujimura, Y. Homma, S. Inoue and J. Yanagisawa, Estrogen Exhibits a Biphasic Effect on Prostate Tumor Growth through the Estrogen Receptor β-KLF5 Pathway, *Mol Cell Biol* **36** (2016), 144–156. doi: 10.1128/MCB.00625-15.

[39] P. Guo, C.S. Xing, X.Y. Fu, D.L. He and J.T. Dong, Ras inhibits TGF-β-induced KLF5 acetylation and transcriptional complex assembly via regulating SMAD2/3 phosphorylation in epithelial cells, *J Cell Biochem* **121** (2020), 2197–2208. doi: 10.1002/jcb.29443.

[40] Y.X. Zhou, X.L. Tang, Z. Huang, J.B. Wen, Q.X. Xiang and D.H. Liu, KLF5 promotes KIF1A expression through transcriptional repression of microRNA-338 in the development of pediatric neuroblastoma, *J Pediatr Surg* **57** (2022), 192–201. doi: 10.1016/j.jpedsurg.2021.12.020.

[41] D. Ma, L.Y. Chang, S. Zhao, J.J. Zhao, Y.J. Xiong, F.Y. Cao, L. Yuan, Q. Zhang, X.Y. Wang, M.L. Geng, H.Y. Zheng and O. Li, KLF5 promotes cervical cancer proliferation, migration and invasion in a manner partly dependent on TNFRSF11a expression, *Sci Rep* **7** (2017), 15683. doi: 10.1038/s41598-017-15979-1.

[42] J. Cancelas, C.P. Zhang, A. D'Alessandro, A. Wellendorf, F.

Mohmoud, B. Dasgupta, J. Whitsett and H.L. Grimes, Klf5 Deficiency Is Required for B-Cell Lymphoid Progenitor Leukemogenesis to Promote Glutathione Biosynthesis and Prevent Oxidative Stress, *Experimental Hematology* **44** (2016), S62–S62. doi: 10.1016/j.exphem.2016.06.103.

[43] L. Sun, X.N. Zhou, Y.M. Li, W. Chen, S.N. Wu, B. Zhang, J.Y. Yao and A.J. Xu, KLF5 regulates epithelial-mesenchymal transition of liver cancer cells in the context of p53 loss through miR-192 targeting of ZEB2, *Cell Adh Migr* **14** (2020), 182–194. doi: 10.1080/19336918.2020.1826216.

[44] B.T. Zhang, Z.Q. Zhang, S.Y. Xia, C.S. Xing, X.P. Ci, X. Li, R.R. Zhao, S. Tian, G. Ma, Z.M. Zhu, L.Y. Fu and J.T. Dong, KLF5 Activates MicroRNA 200 Transcription To Maintain Epithelial Characteristics and Prevent Induced Epithelial-Mesenchymal Transition in Epithelial Cells, *Mol Cell Biol* **33** (2013), 4919–4935. doi: 10.1128/MCB.00787-13.

[45] R.C. Qi, J.Y. Wang, Y.M. Jiang, Y. Qiu, M. Xu, R.M. Rong and T.Y. Zhu, Snai1-induced partial epithelial-mesenchymal transition orchestrates p53-p21-mediated G2/M arrest in the progression of renal fibrosis via NF-κB-mediated inflammation, *Cell Death Dis* **12** (2021), 44. doi: 10.1038/s41419-020-03322-y.

[46] K. Lu, J.L. Dong and W.J. Fan, Twist1/2 activates MMP2 expression via binding to its promoter in colorectal cancer, *Eur Rev Med Pharmacol Sci* **22** (2018), 8210–8219. doi: 10.26355/eurrev_201812_16514.

[47] A.V. Timofeeva, I.S. Fedorov, A.V. Asaturova, M.V. Sannikova, A.V. Tregubova, O.A. Mayboroda, G.N. Khabas, V.E. Frankevich and G.T. Sukhikh, Blood Plasma Small Non-Coding RNAs as Diagnostic Molecules for the Progesterone-Receptor-Negative Phenotype of Serous Ovarian Tumors, *Int J Mol Sci* **24** (2023), 12214. doi: 10.3390/ijms241512214.

[48] X.Y. Yang and W.P. Zhu, ERBB3 mediates the PI3K/AKT/mTOR pathway to alter the epithelial-mesenchymal transition in cervical cancer and predict immunity filtration outcome, *Exp Ther Med* **25** (2023), 146. doi: 10.3892/etm.2023.11845.